

Preparation of Br-terminated Si(100) and Si(111) surfaces and their use as ALD resists

Running title: Silicon bromination to prepare an ALD resist

Running Authors: Mason and Teplyakov

John R. Mason¹ and Andrew V. Teplyakov^{1,a)}

¹ Department of Chemistry and Biochemistry, University of Delaware, Newark, Delaware, 19716, USA

a) Electronic mail: andrewt@udel.edu

Abstract

In area selective processes, such as area-selective atomic layer deposition (AS-ALD), there is renewed interest in designing surface modification schemes allowing to tune the reactivity of the non-growth (NG) substrates. Many efforts are directed towards small molecule inhibitors (SMI) or even atomic layers, which would modify selected surfaces to delay the nucleation and provide the NG properties in the target AS-ALD processes and at the same time would have the size that is substantially smaller than the features produced with this approach. Bromine termination of silicon surfaces, specifically Si(100) and Si(111), is evaluated as a potential pathway to design NG substrates for deposition of metal oxides, and TiO₂ (from cycles of sequential exposures of tetrakis-dimethylamidotitanium (TDMAT) and water) is tested as a prototypical deposition material. The nucleation delays on the surfaces produced are comparable to those on the H-terminated silicon that is commonly used as a NG substrate. However, the silicon surfaces produced by bromination are more stable, and even oxidation does not change their chemical reactivity substantially. Once

the NG surface is eventually overgrown after a large number of ALD cycles, bromine remains at the interface between silicon and TiO₂. The NG behavior of different crystal faces of silicon appears to be similar despite different arrangement and coverage of bromine atoms.

Keywords: silicon, surface bromination, ALD resist

I. INTRODUCTION

Surface modification of semiconductors has become a cornerstone of modern bottom-up strategies to advance microelectronics to the limit of and beyond Moore's law¹. Self-aligned approach to nanofabrication requires processing that is conformal and highly selective, and this is where semiconductor functionalization provides chemical pathways to produce versatile surfaces that can act as a guide for chemical reactivity promoting deposition of desired materials or delay the nucleation leading to high resistance for depositing undesired materials on patterned substrates, so called area-selective deposition. Atomic layer deposition (ALD), where films with atomically precise thickness are deposited using complementary self-saturating half-cycle processes, is a key technology for modern control of the feature size in microelectronics, and combining the properties of modified surfaces with fundamental understanding of the deposition processes leads to the development of area-selective ALD or AS-ALD^{2,3}.

While a large number of reviews are dedicated to AS-ALD, a recent paper by Mameli and Teplyakov⁴ explicitly summarized the different combinations of growth and non-growth surfaces and compared the inherently selective combinations of substrates with those using protection by chemical modification and additional physical pretreatment methods (such as plasma-based ones). Among all these venues, the most recent developments concern applications of small molecule

inhibitors (SMI) and even atomic layer resists. It is worth mentioning that surface modification to produce deposition-resistant monolayer can be utilized either prior to ALD or be included as one of the repeating steps in the process. This manuscript will focus on a starting point that can be accessed using simple solution-based surface modification of silicon surfaces and compare the properties of Si(100) and Si(111) starting substrates.

Silicon surface chemistry has been investigated heavily and reviewed substantially over nearly half a century, because of the utility of this material in microelectronics since the invention of the transistor. That is why silicon chemistry still remains to be in demand, and its new connections to applications in AS-ALD⁵⁻⁸ are always needed.

Currently, most of AS-ALD work utilizes hydrogen-, hydroxyl- or (more rarely) chlorine-terminated silicon surfaces. Each of these terminations is well defined and shown to work as a resist in some combinations with ALD-deposited materials; however, these substrates also have a number of issues, specifically, thermal and chemical stability and reactivity with a wide number of precursor molecules, limiting the application to only some specific combinations of chemicals.

Chlorine termination for silicon surfaces is commonly used as either a resist for deposition or as a precursor for further modifications^{9,10}. Some recent work also suggests that Br-terminated surfaces could serve as robust, stable, and versatile resists. In selected cases, a nearly perfect Br-terminated silicon surface could be produced, but the well-ordered and well-understood Br-Si(100) can only be prepared in ultra-high vacuum (UHV) conditions, as shown by Butera¹¹, and while it shows exceptional stability in ambient conditions, with little oxidation for up to eight hours in ambient, the procedure is complicated and costly for commercial application. Outside UHV, only a few silicon bromination procedures have been reported. The main one is based on Br₂ solution in alcohol for electrical passivation of silicon with potential applications in solar cells. A paper by

Batra et al.¹² and multiple references therein describe not only successful use of this approach for Br-termination of silicon, but also compare the electrical properties for a number of substrates treated with other chemical methods, including iodination. However, chemical and electrical passivation are not necessarily referring to the same surface species produced by chemical treatments, and in the case of liquid bromination with ethanol solution, the starting material, preparation methods, possible oxidation and even the chemistry of surface modification do not result in a fully brominated and uniform surface, despite reasonably high reported bromine coverage¹³. Thus, this approach may indeed result in excellent electrical properties of the resulting surface, but is unlikely to provide an efficient NG substrate for ALD. A report by Eves and Lopinski¹⁴ utilized a nearly perfect monohydride-covered Si(111) exposed to gas-phase bromine at ~200 Torr to produce a very high-coverage Br-Si(111) substrate, as was confirmed by scanning tunneling microscopy, and the work by He et al. used liquid-phase modification of H-Si(111) with N-chloro- and N-bromosuccinamide to produce stable halogenated silicon surfaces¹⁵. However; neither work attempted to investigate the (100) face or evaluate the possible applications of any brominated surfaces as potential deposition resists. Finally, one recent study by Raffaelle et al² used gas-phase reaction of N-bromosuccinimide with H-terminated Si(100) substrate to create a bromine terminated silicon surface and utilized it as a resist for atomic layer deposition (ALD), however this procedure still involves medium vacuum conditions (10^{-3} Torr) and may lead to organic contamination. Thus, new schemes for surface modifications are still needed.

This work provides a procedure for liquid phase bromination of Si(100) and Si(111) with Br_2 solution in methylene chloride and tests the produced surfaces as resists for ALD of TiO_2 with tetrakis-dimethylamido-titanium and water (as a co-reagent) in thermal ALD cycles.

The surfaces produced by this approach are stable but can act as a resist as effective as those based on hydrogen terminations. They can also be used for further modifications and/or bromine removal for future applications. In fact, the silicon-bromine bond energy (343 kJ/mol) is substantially lower than that for a silicon-chlorine bond (456 kJ/mol)¹⁶, showing that it may allow for easier removal as compared to chlorine-terminated silicon for further modifications. Despite this apparent disadvantage for a potential ALD resist, Br-terminated silicon substrates have been proven to be very effective because of the size of the bromine atom, even for partially oxidized surfaces. This hypothesis was suggested both for the UHV-prepared nearly ideal Br-Si(100) surfaces¹⁷ and for the silicon surfaces treated with gas-phase N-bromosuccinimide².

A direct comparison of (100) and (111) faces of silicon single crystal terminated with halogens is rare. For example, although Sekar et al.¹⁸ have attempted to compare the stability of Br-Si(100) and Br-Si(111) prepared by reacting H-terminated silicon with liquid phase Br₂ in methanol. The reported data suggest that the surfaces had mixed species, presence of hydrogen and affected by oxidation, as would be expected for this preparation method. The comparison of (100) and (111) Br-functionalized surfaces of silicon as resists for ALD has never been performed previously. The main argument is that the technologically-relevant Si(100) surface is the primary target because of its atomically flat interface with oxide. However, Si(111) functionalized with atomic-level precision can also be a viable option in AS-ALD, and thus it is important to compare the chemical reactivity in realistic ALD conditions for these two functionalized crystal faces of silicon, which is evaluated in this work.

Finally, any NG surface eventually loses its selectivity compared to the growth substrate, which brings up a question of what happens to the modifier molecule or atom. Does it remain at

the silicon/oxide interface or does it diffuse throughout the layered structures? Spectroscopic techniques and depth profiling are utilized here to show that bromine atoms remain at the interface.

II. EXPERIMENTAL

A. Materials

For this study, double side polished Si(100) wafers (p-doped, Virginia Semiconductors, $400 \pm 25 \mu\text{m}$, $1\text{-}10 \Omega - \text{cm}$ resistivity) and single side polished Si(111) (p-doped, University Wafers, $280 \mu\text{m}$, $0.001 - 0.005 \Omega - \text{cm}$ resistivity) were used for subsequent modifications. Deionized water with $18 \text{ M}\Omega\text{ cm}$ resistivity was taken from a first-generation Milli-Q water system (Milipore). Hydrogen peroxide (Fisher, 30 % certified ACS grade), ammonium hydroxide (Fisher, 29 % certified ACS grade), hydrochloric acid (Fisher, 37.3 % certified ACS grade), buffered oxide etchant (BOE) 6:1 (Fisher Chemical), methylene chloride (Sigma Aldrich, 99.8 %, anhydrous), bromine (Sigma Aldrich 99.5 % ACS reagent) were used without additional preparation. Nitrogen used for purging the reaction and drying samples was from boil-off from a liquid nitrogen tank.

B. Preparation procedures

1. Preparation of hydroxyl and hydrogen terminated Si(100) and Si(111)

The silicon wafers were cut and cleaned using a modified Radio Corporation of America (RCA) method¹⁹. The Teflon beakers were cleaned using a solution of standard cleaning-1 (SC-1) by preparing a solution of four parts Milli-Q ultra-pure water, one part hydrogen peroxide, and one part ammonium hydroxide, and placed in an 80°C water bath for 30 minutes. Silicon wafers were cleaned in the freshly prepared SC-1 solution for 10 minutes at 80°C . The wafers were then rinsed

with Milli-Q water before etching. Then, the wafers were etched for 2 minutes in the buffer solution of hydrofluoric acid and rinsed with Milli-Q water. Next, samples were placed into a solution of 4-1-1 by volume of Milli-Q ultra-pure water, hydrogen peroxide and hydrochloric acid. This is used to prepare the hydroxyl-terminated silicon surfaces that are used for ALD later in the experiment or to further produce H-terminated silicon surfaces. For hydrogen termination, the substrates are rinsed again and etched a second time in the HF buffer solution for 1 minute, followed by a brief rinse and 6-minute etching in ammonium fluoride and rinsed again with water.

2. Preparation of bromine-terminated Si(100) and Si(111)

The freshly prepared H-Si substrates were quickly rinsed with methylene chloride and placed into a solution of 10 mL of methylene chloride and 0.5 mL of liquid bromine (9.7 μ M) and then placed under nitrogen at room temperature and allowed to react for the predetermined time (up to 2 hours). After the time period, samples were rinsed in methylene chloride and dried under nitrogen, before ALD and further analysis.

3. ALD of TiO₂ on hydroxyl- and bromine-terminated Si(100) and Si(111)

Once the samples were prepared, they were placed into a commercial Oxford FlexAL II Thermal/Plasma ALD chamber after brief exposure to ambient. The ALD chamber base pressure was 7×10^{-9} Torr, and a thermal recipe for TiO₂ at 130 °C was used. Each cycle consisted of TDMAT dose for 1 s followed by 10 s argon (Ar) purge, 3 s vacuum pumping, 20 ms of H₂O pulse and 10 s of Ar purge, pumped for 1 min, then the cycles were repeated. All reactants were delivered with 200 SCCM Ar and purged with 100 SCCM Ar.

C. Characterization techniques

1. X-ray photoelectron spectroscopy (XPS)

XPS was performed on a Thermo Scientific K-Alpha+ equipped with an Al K α source ($h\nu = 1486.6$ eV). The base analysis pressure is 4×10^{-9} torr and take-off angle of 35.3° with respect to the analyzer. The survey spectra were recorded for energy range of 0 – 1000 eV, with a pass energy of 200 eV, and a step size of 1 eV with dwell time of 10 ms. High-resolution spectra were collected for C 1s, O 1s, Si 2p, Ti 2p, and Br 3d regions with a pass energy of 50 eV, step size of 0.1 eV and dwell time of 50 ms. Data was analyzed with CASAXPS software (version 2.3.25) and calibrated using C 1s at 284.6 eV. Fitting of the Br 3d spectral regions was performed with a mixture of Gaussian and Lorentzian line shapes using CASAXPS software, and the two spin-orbit coupled peaks were separated by 1.05 eV, with restrictions for full width at half max and constrained area ratios of 3-to-2 for the 5/2 and 3/2 spin-orbit coupled components, and using Shirley background correction.

2. Time-of-flight secondary ion mass spectroscopy (ToF-SIMS)

The ToF-SIMS analysis was performed on a TOF.SIMS 5 instrument (IONTOF USA, Inc.) equipped with a Bi_n^{m+} ($m = 1,2$ & $n = 1-5$) liquid metal ion gun, low energy electron flood gun for charge compensation and, a dual-source O₂ and Cs ion column for low energy sputtering. For depth profiling, an energy of 500 eV Cs⁺ sputter ion beam with a 30 nA current was applied to a 200 x 200 μm^2 area, with a 50 x 50 μm^2 area for analysis at the center of the sputter crater, analyzed with a pulsed 30 keV, 0.13 pA Bi⁺ primary ion beam. During the analysis, the negative ions were collected and calibrated using mass-to-charge ratios for C⁻, C₂⁻, C₃⁻, CH⁻, CH₂⁻, CH₃⁻, and C₂H⁻. Data was then analyzed using ionTOF's SurfaceLab (version 7.3) base data analysis package.

3. Atomic force microscopy (AFM)

AFM images were recorded using an Anasys Nano IR2 system, in tapping mode. Gold-coated, microfabricated silicon probes that were ~ 225 μm long, and pre-mounted on half-waster mounts were acquired from Bruker. Images were processed using GWIDDION software (version 2.66) to evaluate surface roughness.

D. Computational details

Computational modeling was performed using Density Functional Theory (DFT) calculations in Gaussian 16²⁰ suite programs, with B3LYP functional and 6-311+G(d,p) basis set with Grimme's D3 dispersion corrections^{21,22} (empiricaldispersion = gd3). The silicon clusters used to represent Si(100) surface, were Si₂₁H₂₄, with silicon and hydrogen atoms in lower three layers fixed at their bulk positions to prevent unrealistic distortions of cluster models. The silicon clusters used to represent the unreconstructed Si(111) surface, were Si₁₇H₂₄, with silicon and hydrogen atoms in lower three layers fixed at their bulk positions to prevent unrealistic distortions of cluster models. For the reactions, a monohydride, mono-hydroxyl and monobromide species were used as ideal and representative models. While these surfaces only describe specific surface sites rather than all the available surface functionalities and reconstructions, they are indeed representing a substantial portion of possible surface reactive sites, and the comparison of reactivity of (100) and (111) silicon faces. For adsorption studies, a tetrakis-dimethylamidotitanium molecule was optimized before being placed 3 – 5 \AA away from the surfaces and allowed to optimize. Same computational approaches and cluster models have been successfully used previously in studies of surface modification and atomic layer deposition

processes^{10,23,24}. The cartesian coordinates of all the models used in this work are resented in the Supplementary Material section.

III. RESULTS AND DISCUSSION

Figure 1 shows the steps followed for the preparation of OH-Si and Br-Si surfaces. Once prepared, these surfaces were compared for ALD process with subsequent exposure to TDMAT and H₂O self-limiting half-cycle reactions at 130 °C, as also indicated in the figure. After each set of ALD cycles, the samples were loaded into the XPS chamber with minimal exposure to ambient for analysis as described below or used for other characterization.

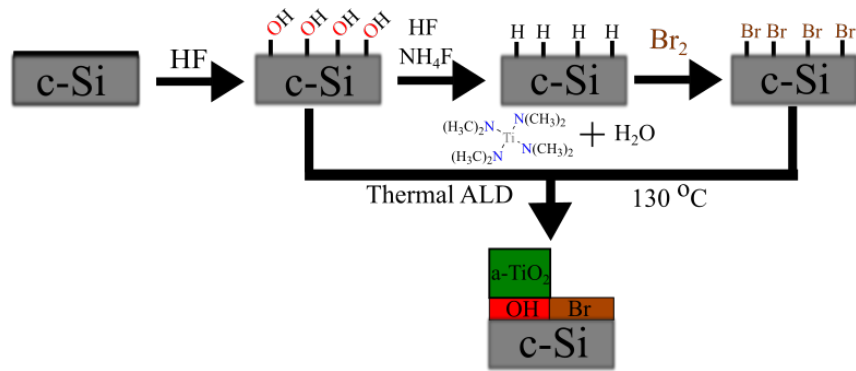
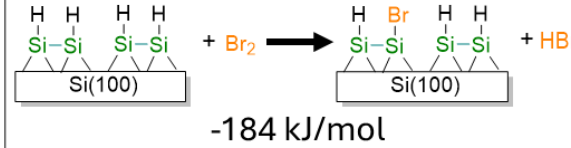
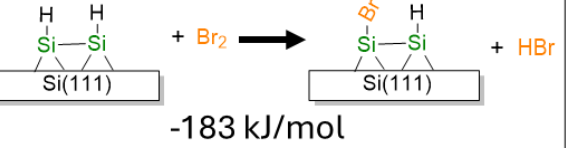
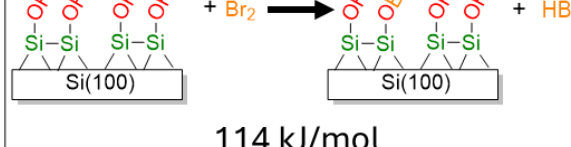


Figure 1 Schematic representation of steps followed in the preparation of OH-, H-, and Br-terminated Si(100) and Si(111) surfaces used in the comparison of TiO₂ growth by ALD.

A. Computational investigation

Before experimental investigation, computational studies helped establish the reasonable pathways for surface modification by bromine and further potential reactions with TDMAT.

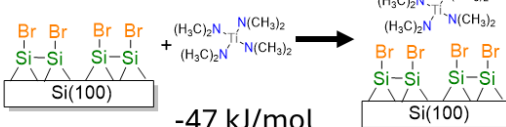
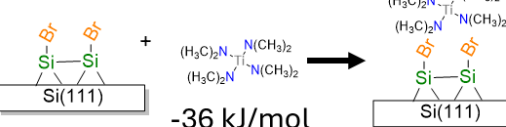
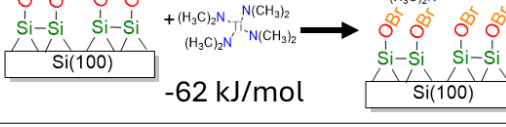
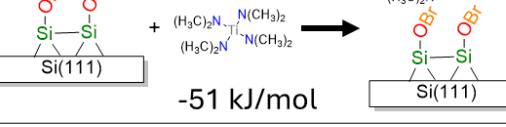
Table 1 Summary of the DFT computational predictions for the thermodynamic requirements for the reaction of Br_2 with H- and HO- terminated Si(100) and Si(111) surfaces represented by cluster models.

Si(100)		Si(111)
H	 <p>-184 kJ/mol</p>	 <p>-183 kJ/mol</p>
OH	 <p>114 kJ/mol</p>	 <p>107 kJ/mol</p>

The computational results summarized in Table 1 show that the reaction of Br_2 with both H-terminated silicon surfaces is exothermic. In fact, the thermodynamic requirements for the formation of the Si-Br bond in these transformations are nearly identical for monobromide species on Si(100) and Si(111) crystal faces. At the same time, if the hydroxyl groups are present on either one of them, their reaction with Br_2 appears to be thermodynamically unfavorable. The energy increase upon the formation of -OBr surface species is 114 kJ/mol for Si(100) and 107 kJ/mol for Si(111). Even though these simple cluster models may not represent the variety of species present on a surface, especially for Si(100), they certainly provide some qualitative comparison and apparent similarity in reactivity of the two hydrogen-covered crystal faces of silicon with Br_2 . In other words, the majority of the surface species formed by bromination are oxygen-free. Bromination is certainly possible and leads largely to the formation of Si-Br functionalized surfaces. In addition, if surface defects, such as hydroxyl groups, are present, they are unlikely to

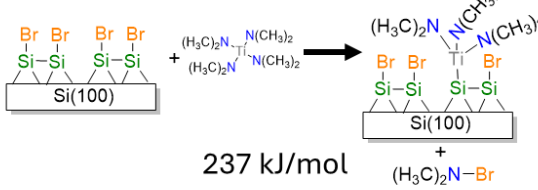
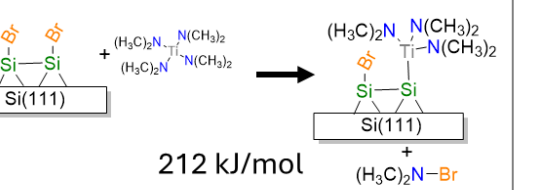
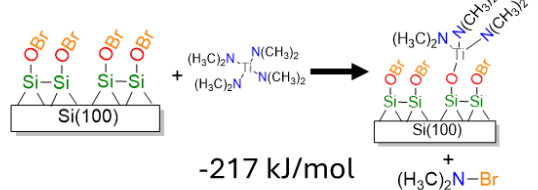
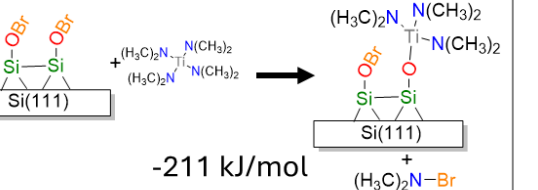
react with Br_2 , and thus silicon surface would be expected to be easily chemically passivated by bromination.

Table 2. Summary of the DFT computational predictions for the thermodynamic requirements for the molecular adsorption of TDMAT on Br- and BrO- terminated Si(100) and Si(111) surfaces represented by cluster models.

Si(100)		Si(111)	
Br	 <p>-47 kJ/mol</p>	 <p>-36 kJ/mol</p>	
OBr	 <p>-62 kJ/mol</p>	 <p>-51 kJ/mol</p>	

In [Error! Reference source not found.](#), a simple DFT analysis of the molecular adsorption of TDMAT on selectively-terminated Si(100) and Si(111) surfaces is shown. TDMAT was initially positioned 3 – 5 Å away from the cluster models representing fully bromine- and fully oxibromide-terminated silicon surfaces, and the energy of the structures produced was minimized. The data in Table 2 show that the interactions between the TDMAT molecule and the surface bromine atoms are mainly governed by the dispersion forces, with slightly stronger molecular adsorption on the oxidized surfaces as compared to the bromine terminated surface.

Table 3. Summary of the DFT computational predictions for the thermodynamic requirements for the initial step of the ALD, following chemisorption of TDMAT on Br- and BrO- terminated Si(100) and Si(111) surfaces represented by cluster models.

	Si(100)	Si(111)
Br	 <p style="text-align: center;">237 kJ/mol</p>	 <p style="text-align: center;">212 kJ/mol</p>
OBr	 <p style="text-align: center;">-217 kJ/mol</p>	 <p style="text-align: center;">-211 kJ/mol</p>

In **In Error! Reference source not found.**, the DFT-predicted thermodynamics of potential reactions of TDMAT with Br-functional groups on silicon surfaces is summarized. One of the bromine atoms was replaced in each structure by the tris-dimethylamidotitanium fragment and optimized, with a biproduct of bromo-dimethylamine. While this biproduct is not the only one possible and certainly many different adsorption configurations could be present on a realistic substrate, these computations allow for the direct comparison of different surface species and reactivities of different silicon crystal faces. The general observation is that chemisorption thermodynamics is very similar on Si(100) and Si(111) surfaces, although local structures could certainly lead to noticeable differences in the stability of different species. For example, the Ti-Si bond length in the tris-dimethylamido titanium species adsorbed on the cluster model representing Si(100) is 2.67 Å, while on Si(111), it is 2.64 Å, which appear to translate in about 25 kJ/mol difference in the stability of surface species produced.

When comparing the reactivity of the oxidized versus the unoxidized bromine surface species, the reactions leading to the formation of the Ti-O bond are much more favorable than those leading to the formation of Ti-Si. This follows a similarly known trend that hydroxyl

terminated surfaces are a better growth surface as compared to hydrogen terminated surfaces¹⁰ and suggests that the formation of surface oxygen-containing defects would ultimately lead to the loss of selectivity on Br-terminated surfaces compared to the growth-promoting substrates.

B. Bromination of Si (100) and (111)

Given the previous reports of silicon bromination and the summary of the preliminary data in the computational studies described above, it was important to evaluate the efficacy of this reaction and compare it on the two most commonly used faces of silicon single crystal experimentally. Thus, silicon (111) and (100) surfaces were first H-terminated, as described above and then the resulting substrates were brominated using 0.5 mL of Br₂ in 10 mL of methylene chloride. These procedures were optimized for minimum surface oxidation with highest consistent coverages.

1. Bromination of Si(100)

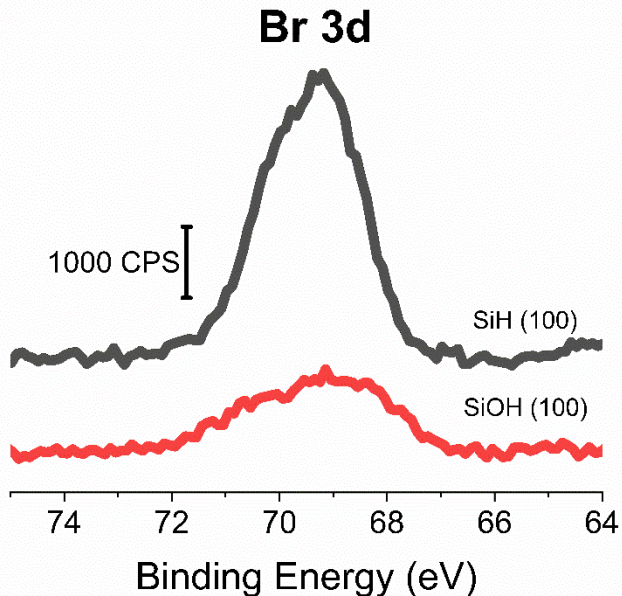


Fig 2. Comparison of the Br 3d spectral regions recorded by XPS after bromination of Si(100) on H-Si(100) and HO-Si(100) surfaces.

First, the bromination procedure was tested on hydrogen and hydroxyl terminated silicon (Si(100)), which would be expected to be more reactive due to inhomogeneity) by reacting both for one hour in the same conditions. Based on the example of modified Si(100) shown in Figure 2, it was demonstrated that in similar bromination conditions, the bromine coverage produced on hydroxyl terminated silicon was approximately 3.5 times lower than that on the same surface terminated with hydrogen. This agrees with the above computational data showing that bromine reacting with hydrogen terminated silicon is more favorable as compared to hydroxyl terminations. If the H-terminated Si(100) surface modified with bromine is left in ambient for several weeks, the Br 3d spectrum of that surface (not shown here) becomes more complex, likely corresponding to various oxidation pathways. Investigating the details of this oxidation process is outside of the

scope of this work. For all these reasons, hydrogen terminated silicon was then used for the later experiments on both Si(100) and Si(111) surfaces.

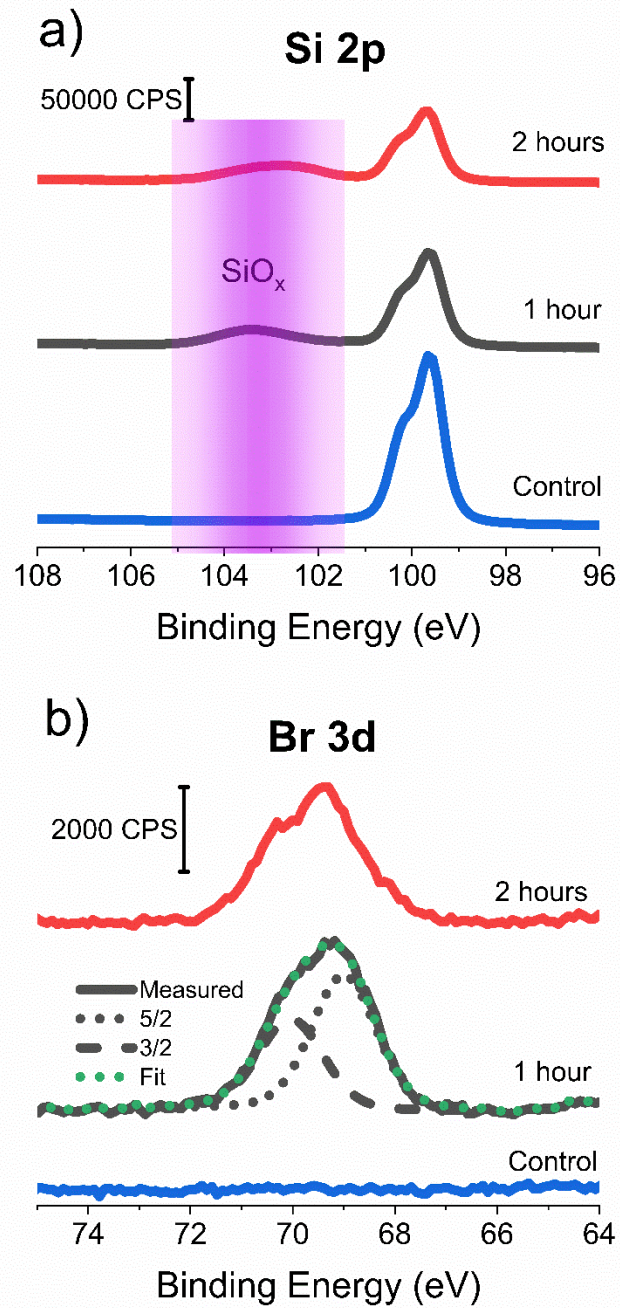


Fig. 3. Comparison of (a) Si 2p and (b) Br 3d spectral regions recorded by XPS after bromination of Si(100) surface after one and two hours of reaction time.

Fig. 3 shows the Si 2p and Br 3d spectral XPS regions for Si(100) after one and two hours of reaction time with liquid solution of bromine in methylene chloride. As shown in the Si 2p spectral region, the starting hydrogen-terminated Si(100) has no observable oxidation. In other words, oxidation could only occur during the bromination process or immediately after. The one- and two-hour samples show oxidation, as evidenced by the presence of the SiO_x feature in the Si 2p spectral region around 103.5 eV. It should be pointed out that the oxidation is also caused by the exposure of the samples to ambient during transfer to the XPS chamber, so the bromine coverage should serve as a better indicator of the efficiency of bromination. Br coverage was quantified based on the previous detailed investigation, where the ideal monobromide-terminated Si(100) surface was prepared in UHV and served as a 100% monolayer covered standard¹¹. Using this approach, and analyzing the intensity ratio for the bromine 3d region to that of the Si 2p spectral features, bromine coverage of $77 \pm 18\%$ (compared to the ideally terminated monobromide) was determined for the 1-hour reaction time, and after two hours the coverage drops to $49 \pm 1\%$ of a monolayer. Peak fitting for the Br 3d experimental spectrum is also shown in Fig. 3. It is expected that the observed features would be heterogeneously broadened. Nevertheless, fitting them with restricted spin-orbit coupling ratio intensities suggests that the observed features could be described by a single pair of peaks, with Br 3d_{5/2} peak positioned at ~ 69.1 eV, which is fully consistent with Si-Br bond present on a surface^{17, 25} rather than Si-OBr. Thus, surface oxidation concerns mostly Si-Si bonds rather than Si-Br, and further investigation can use Si-Br surface groups for further modification or as ALD resist, as described below.

2. Bromination of Si(111)

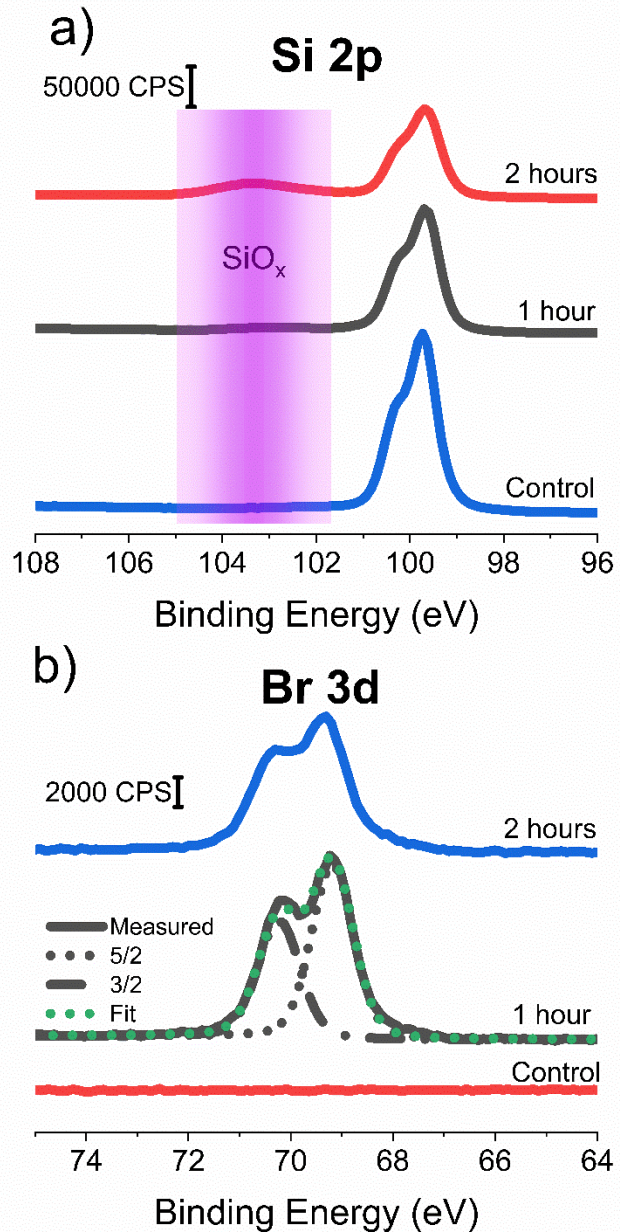


Fig. 4 Comparison of (a) Si 2p and (b) Br 3d spectral regions recorded by XPS after bromination of Si(111) surface after one and two hours of reaction time.

Fig. 4 summarizes the results of bromination of the Si(111) surface. There are some similarities between the two crystal faces, but also there are some notable differences. First, Br-

Si(111) surface is clearly more resistant to oxidation, as no SiO_x features are recorded for 1-hour modification and only a small SiO_x peak is observed for 2-hour reaction. For Br 3d spectral region, Br-Si(111) surface appears to be much more homogeneous compared to the Br-Si(100) substrate. It would be expected based on the nature of the surface species, since Br-Si(100) could be a mixture of monobromide and dibromide species of different orientations and configurations while Br-Si(111) would be expected to be predominantly covered with monobromide species^{17,18}. The peaks corresponding to the spin-orbit split bromine signature on Si(111) have the same positions as those on Br-Si(100); however, they have substantially smaller full-width-at-half-maximum. Overall, the Br 3d features on Si(111) can also be fitted with just one pair of spin-orbit coupled peaks indicating that surface oxidation observed at extended reaction times largely affects the Si-Si bonds and does not lead to the formation of Si-OBr. Another difference between the two crystal faces of silicon is the resulting bromine coverage. In order to evaluate it on Si(111), the intensity ratio for Si 2p/Br 3d features determined for the monobromide terminated Si(100) had to be corrected by the surface density of silicon atoms on the two silicon surfaces. This standard²⁶ was adjusted to account for the additional 13 % of silicon surface atoms on Si(111) face and this corrected value was used for the coverage calculations. Based on this value and analyzing the intensity ratio for the bromine 3d region to that of the Si 2p spectral range, bromine coverage of 98 ± 6 % was determined for the 1-hour reaction time, and after two hours the coverage was 91 ± 3 % of a monolayer. Previous studies by Sekar et al.¹⁸ found that a procedure using a bromine methanol solution (0.05 % by volume) resulted in coverages of 0.62 ± 0.07 monolayer, although it was not specified how the monolayer coverage was defined. In that investigation, according to the preparation method, the surface was almost certainly not nearly atomically flat, and at the best possible coverage degraded readily in ambient.

C. Bromine-terminated silicon as a resist for ALD:

3. Bromine-terminated silicon as a resist for ALD: Si(100)

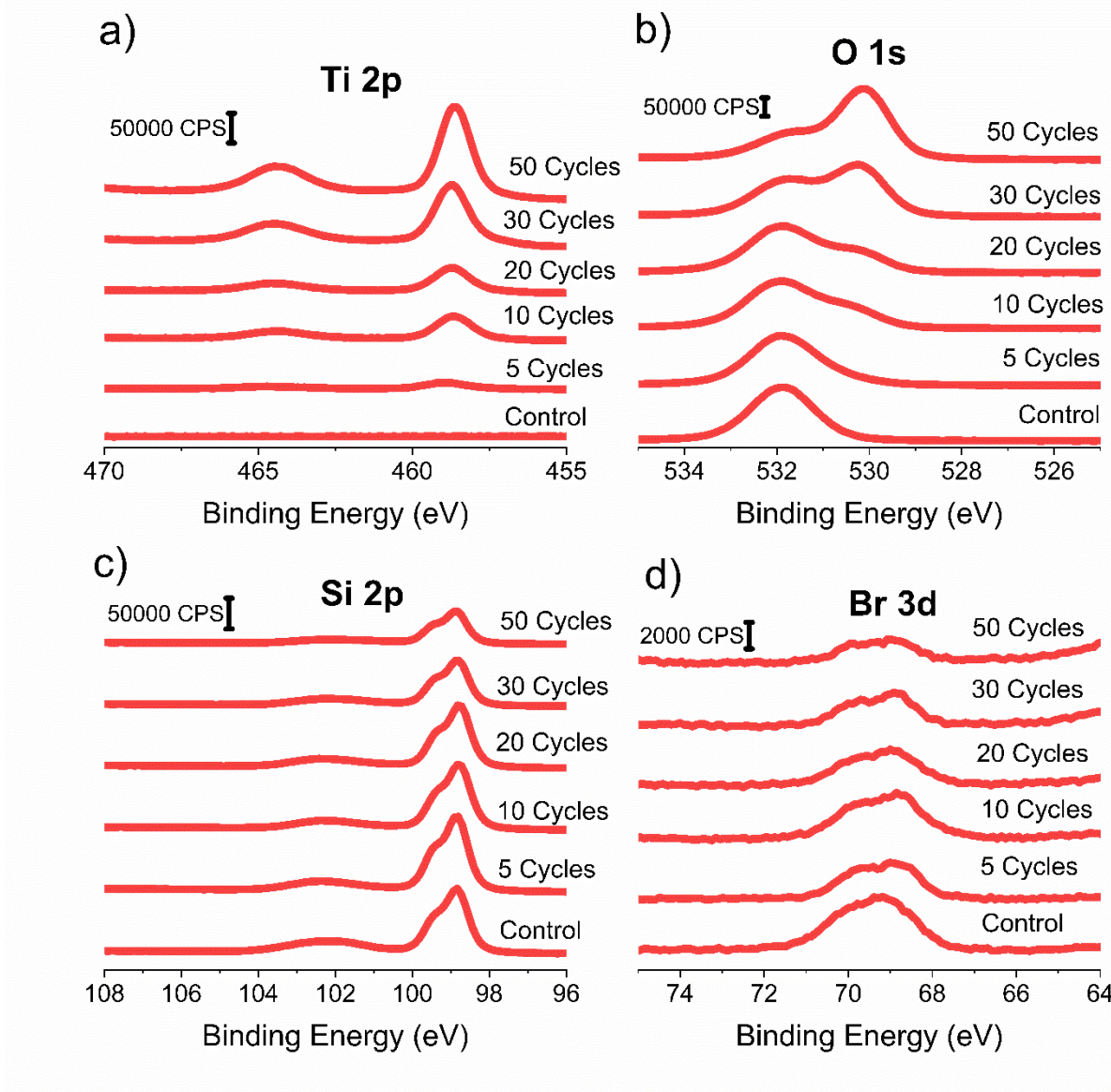


Fig. 5 Ti 2p (a), O 1s (b), and Si 2p (c), Br 3d (d) XPS spectral regions of Br-Si(100) surface recorded after the indicated number of TDMAT/water ALD cycles.

Fig. 5 shows the key XPS spectral regions on Br-Si(100) after 5, 10, 20, 30 and 50 cycles of ALD with TDMAT/water doses. The control sample shows no titanium presence. A very small

amount is being deposited up until the 20-cycle experiment, and then the growth is substantial at 30 and 50 cycles. The Br 3d region shows the same pattern in reverse, where the Br signal does not exhibit significant changes until 30-cycles set, and then the Br 3d intensity decreases, apparently attenuated by the growth of TiO₂. Same behavior is observed for the Si 2p region. Since the samples were briefly exposed to ambient upon the transfer to the XPS chamber, there is always some O-containing species present on the surface. However, the clear peak at ~530-531 eV, the signature of TiO₂ formation^{10,27}, only appears above the 20-cycle growth. The intensity of this peak increases concurrently with the intensity of the Ti 2p features, confirming the TiO₂ growth.

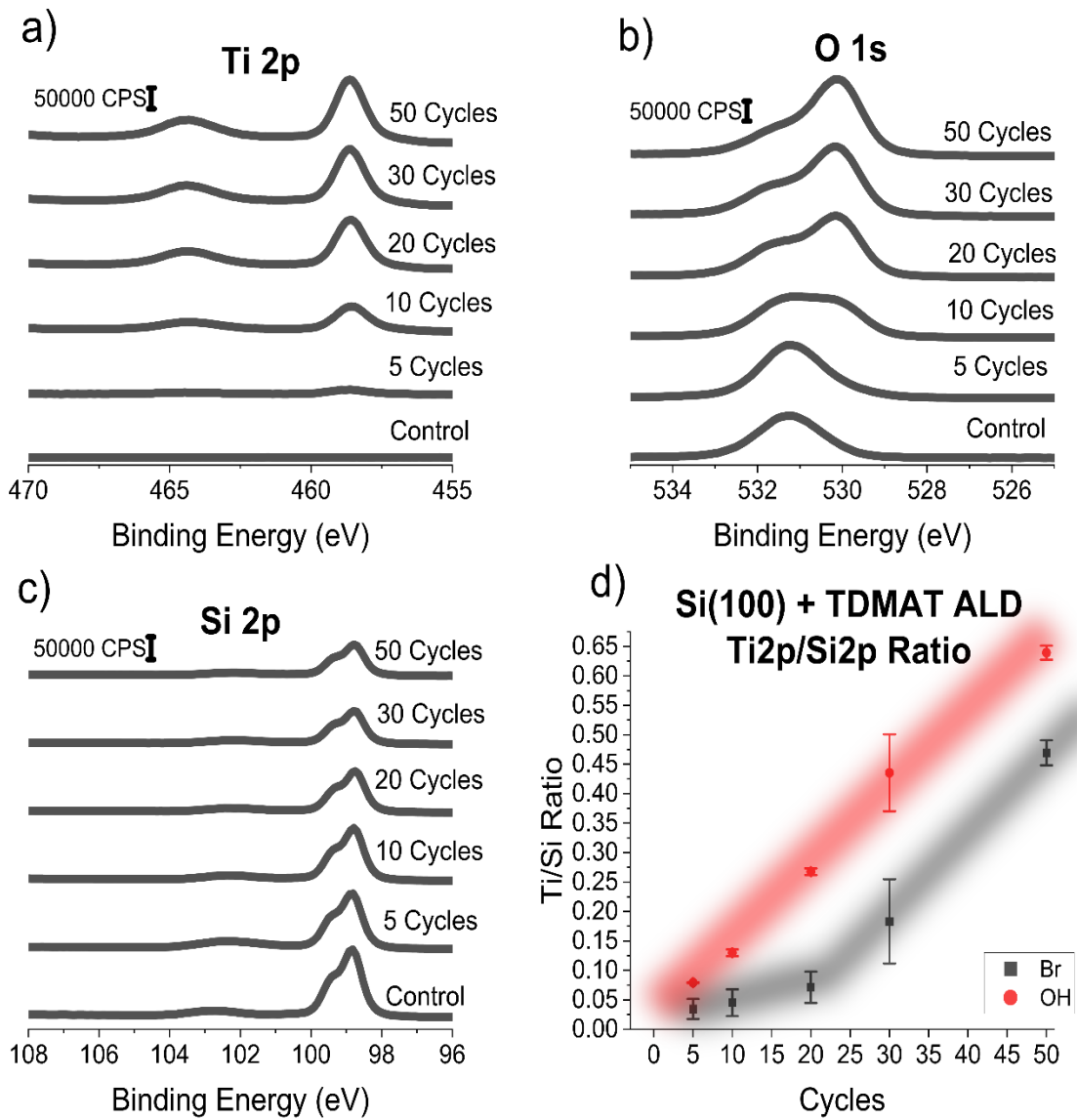


Fig. 6. Ti 2p (a), O 1s (b), and Si 2p (c) XPS spectral regions and Si 2p/Ti 2p ratios (d) for Br-Si(100) and oxidized Si(100) wafer after the indicated number of TDMAT/water ALD cycles.

For comparison, Fig. 6 presents the analysis of the spectral features of the oxidized Si(100) surface as a function of the number of the TiO_2 deposition cycles. This, predominantly hydroxyl-terminated surface shows the expected trends in decreasing silicon and native oxide peaks, while

increasing Ti 2p and the metal oxide O 1s peak gradually with the number of deposition cycles. Panel (d) in this figure compares the deposition of TiO₂ on Br-Si(100) and on the oxidized Si(100) wafer. It is very clear that the oxidized surface promotes TiO₂ deposition and serves as a growth substrate. Br-Si(100) delays the nucleation of the metal oxide until about 30 cycles of ALD, very similarly to what was found previously on H-terminated Si(100) crystal²⁸ and with similar selectivity, approximately 0.51, as defined in Eq 1 in the supporting information up to that point. Following selectivity loss, the growth rate for TiO₂ is essentially the same on both growth and on NG surfaces.

4. Bromine-terminated silicon as a resist for ALD: Si(111)

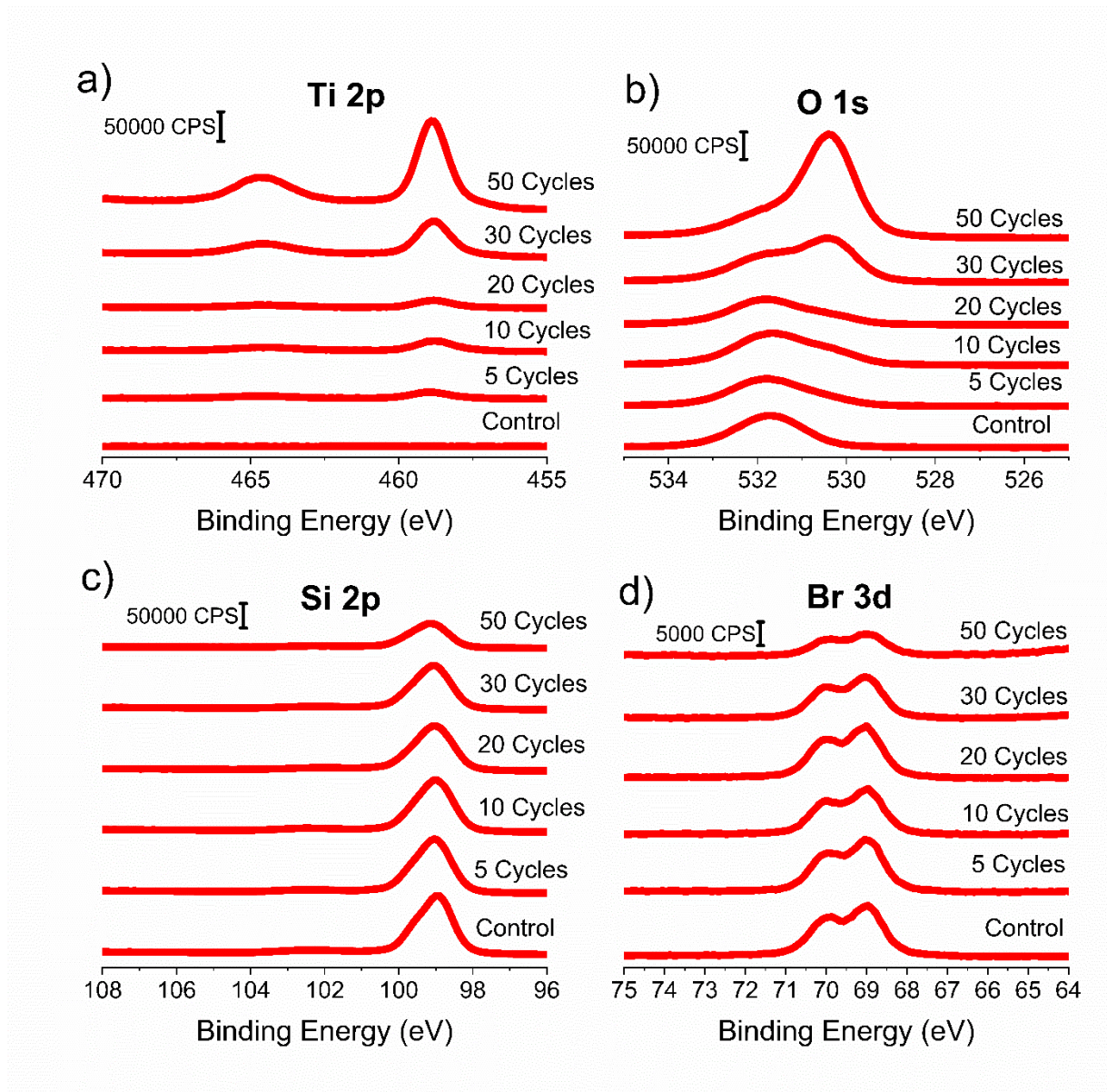


Fig. 7, Ti 2p (a), O 1s (b), and Si 2p (c), Br 3d (d) XPS spectral regions of Br-Si(111) surface recorded after the indicated number of TDMAT/water ALD cycles.

Fig. 7 shows the key XPS spectral regions on Br-Si(111) following 5, 10, 20, 30 and 50 cycles of ALD with TDMAT/water doses. Again, the control sample shows no titanium presence and a very small amount is being deposited until after the 20-cycle experiment. The Br 3d and Si

2p signals are only attenuated by the deposited overlayer of TiO₂ above the 20 cycles. O 1s signature of the metal oxide is only becoming noticeable at 10 cycles and appears prominent above 20 cycles. And the intensity of O 1s (the metal oxide peak at ~530 eV) and Ti 2p increase concurrently, confirming the TiO₂ growth. Figure 8 summarizes the results of the ALD experiment on the oxidized Si(111) surface. Although the native oxide is likely very similar on both silicon faces investigated, it is not necessarily identical, so it is important to show that the growth of TiO₂ on the oxidized Si(100) and Si(111) surfaces is consistently the same, which is indeed the case.

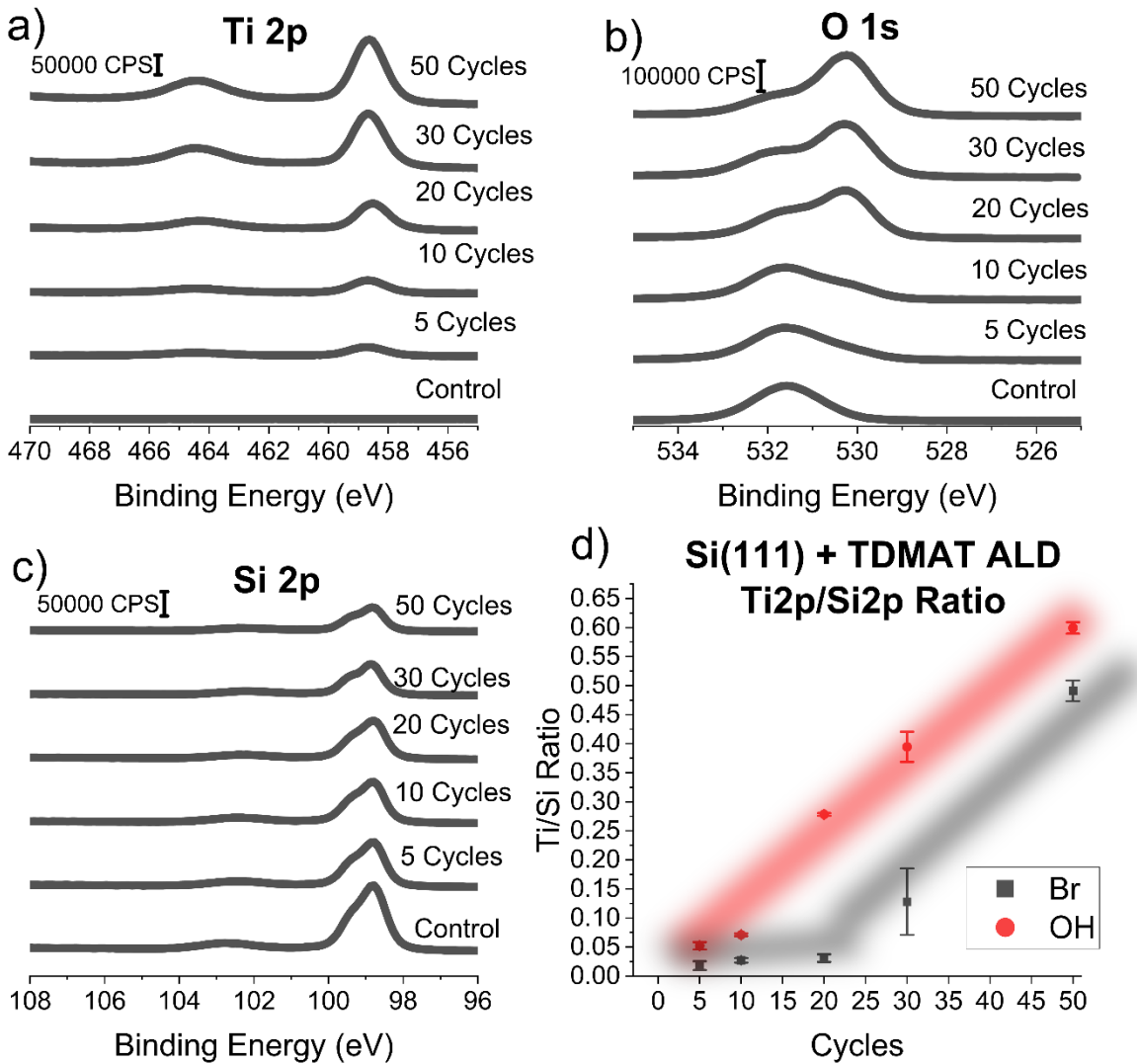


Fig. 8, Ti 2p (a), O 1s (b), and Si 2p (c) XPS spectral regions and Si 2p/Ti 2p ratios (d) for Br-Si(111) and oxidized Si(111) wafer after the indicated number of TDMAT/water ALD cycles.

Again, similarly to the results for Si(100) surface, panel (d) in Fig. 8 compares the bromine- and hydroxyl- terminated Si(111) after ALD. It is apparent that the growth on the oxidized Si(111) surface is nearly linear, while the Br-Si(111) surface delays the nucleation for about 20 cycles. After these 20 cycles, when the selectivity is lost, the deposition catches up to the deposition of

hydroxyl terminated silicon. For these samples, given the high bromine coverage this could suggest that the growth observed is mainly due to defect sites (such as hydroxyl groups) and not from growing on Si-Br entities.

Comparing Si(100) and Si(111), the Si(111) shows high deposition resistance for the first 20 cycles, and then starts to lose selectivity. While the deposition starts to pick up after 20 cycles, the growth rate only catches up with the hydroxyl growth surface for larger number of ALD cycles. Up to this loss of selectivity, the selectivity of Br-Si(111) is nearly 0.62 which is even better than for Br-Si(100). Thus, both Br-Si(100) and Br-Si(111) act as resists towards TiO₂ ALD. Despite heterogeneity and possibly lower bromine coverage per a surface silicon atom, Br-Si(100) appears to act as an efficient resist with very similar behavior to that of the better ordered Br-Si(111).

D. TOF-SIMS analysis of fully encapsulated bromine terminated silicon

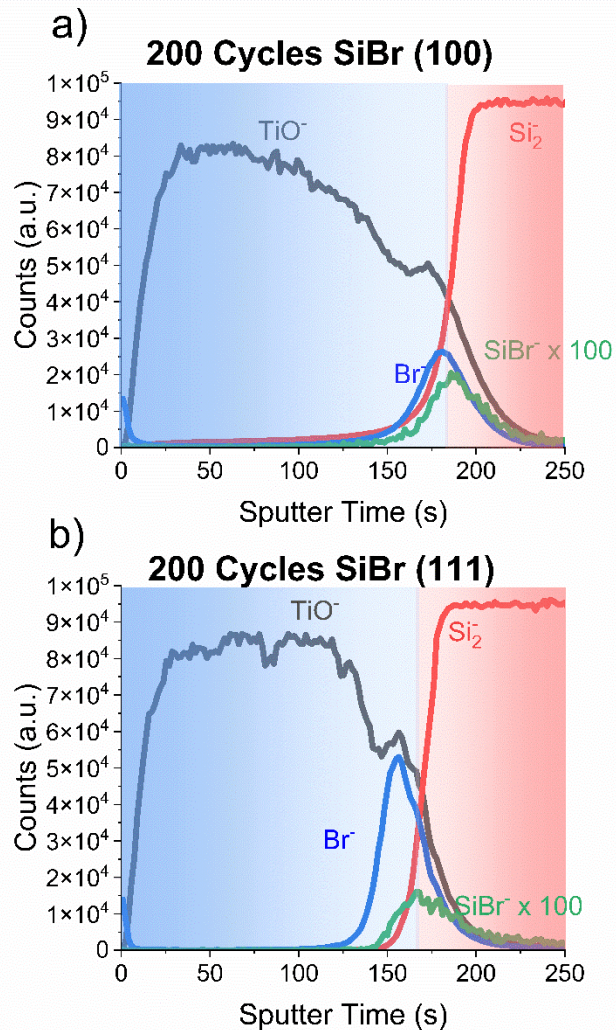


Fig. 9 TOF-SIMS depth profile of Br-terminated a) Si(100) and b) Si(111) following 200 cycles ALD with TDMAT/water.

Once the selectivity is lost and Br-terminated silicon surface is coated with a layer of TiO₂, it is becoming important to answer the question what happens with bromine and if it remains at the interface between silicon and TiO₂. This question needs to be addressed for a number of reasons. Although the AS-ALD is the most obvious application of the Br-terminated silicon surfaces, it has also been shown previously that halogens could be useful for altering the electronic properties, such as minority carrier lifetime, in semiconductors as predicted by Batra et al. on

silicon¹². Silva-Quinones et al.²⁸ has pointed towards the potential of using this strategy for monolayer doping. Their work demonstrated that a silicon surface modified with fluorophenyl boronic acid can be used as a NG substrate for TiO₂ deposition, but once the selectivity is lost and the organic modifier is eventually overgrown with metal oxide, the organic fragment and the boron dopant remain at the Si/TiO₂ interface. In fact, the organic modifier functionality was shown to remain intact underneath the 10 nm thick TiO₂ layer. On the other hand, Ni et al. demonstrated that the decomposition of fluorinated ligands on the surface of CVD-deposited TiO₂ resulted in a distribution of fluorine within the entire TiO₂ layer²⁹. Thus, it is imperative to understand what happens with bromine following the selectivity loss of Br-Si surfaces.

The ToF-SIMS depth profiles of bromine terminated silicon shown in Fig. 9 were evaluated on both Br-Si(100) and Br-Si(111) after 200 cycles of ALD with TDMAT and water. In a previous set of investigations with 4-fluorophenylboronic acid-modified Si(100) sample, it also took approximately 20 ALD cycles at the same conditions for the NG surface to loose selectivity, and the resulting TiO₂ layer reached approximately 10 nm after 200 ALD cycles. Thus, the Si/TiO₂ interface shown in Figure 9 for both crystal faces is covered by approximately 10 nm of metal oxide, although the x-axis is provided in the units of sputtering time. To make sure that the resulting ToF-SIMS depth profiles are not affected by surface roughness, AFM investigations summarized in Figures S1-S3 in the Supplementary Material section were performed and showed that both the starting surfaces and the substrates following 200 cycles of ALD are quite flat, with RMS = 1.0 and 0.98 nm, respectively. Further work will be needed to describe the details of surface nucleation process, but for the moment, it is sufficient to confirm that the results of ToF-SIMS investigation are not affected by surface roughness. Figure 9 plots the depth profile for secondary ions of TiO⁻ to track titanium dioxide, ⁷⁹Br⁻ for bromine, and Si₂⁻ for the bulk silicon.

Both surfaces show that the bromine stays at the interface even after the selectivity is lost and the surface is fully overgrown. Although the data collected by ToF-SIMS are semiquantitative, Figure 9 also provides the confirmation that Si-Br species still exist on that interface following the loss of selectivity. The different intensity ratios for Br^- and SiBr^- species on (100) and (111) silicon crystals suggest that Br-containing entities at the TiO_2/Si interface are different on these two crystal faces.

IV. CONCLUSIONS

Bromination of Si(100) and Si(111) surfaces was achieved as a result of liquid phase modification of respective H-terminated crystal faces with Br_2 solution in methylene chloride. The resulting surfaces showed high coverage of bromine and stability in ambient, if the bromination conditions are properly optimized. Partial surface oxidation did not appear to affect the Si-Br bonds but rather resulted in oxidation of Si-Si bonds. The experimentally observed reactions were compared with the results of DFT calculations.

Both Br-Si(100) and Br-Si(111) surfaces were evaluated as potential resists in AS-ALD of TiO_2 based on the ALD cycles using TDMAT and water, and both surfaces exhibited selectivity that is similar to that of previously reported H-Si(100) compared to the oxidized silicon wafers, and the selectivity for Br-Si(111), 0.62, was higher than that for Br-Si(100), 0.51 for up to 20 deposition cycles.

Following the eventual loss of selectivity, the Br-Si substrates are overgrown with TiO_2 ; however, ToF-SIMS investigations confirmed that bromine remains at the Si/TiO_2 interface and SiBr bond still exists in the final layered structure.

This work provides a new approach for silicon surface modification for a variety of applications, from AS-ALD to monolayer doping, and offers the comparison of reactivity and stability of Br-Si(100) and Br-Si(111) crystal faces.

SUPPLEMENTAL MATERIAL

See supplementary material at [URL will be inserted by AIP Publishing] for AFM images of the starting surfaces and the same surfaces following ALD, equation for calculating the selectivity of non-growth surfaces with respect to the growth surfaces, and computational structures investigated.

ACKNOWLEDGMENTS

This work was supported by the National Science Foundation (CMMI-2225900). The XPS and ToF-SIMS experiments were performed with the instruments sponsored by the National Science Foundation under grant Nos. CHE-1428149 and DMR-2116754.

AUTHOR DECLARATIONS

Conflicts of Interest

The authors have no conflicts to disclose.

DATA AVAILABILITY

The data that support the findings of this study are available within the article and in the extensive supporting information section. Additional spectroscopic and microscopic data are available upon request.

REFERENCES

¹ F. Iacopi, and F. Balestra, “More-than-Moore Devices and Integration for Semiconductors,” (Springer International Publishing, 2023).

² P.R. Raffaelle, G.T. Wang, and A.A. Shestopalov, “Vapor-Phase Halogenation of Hydrogen-Terminated Silicon(100) Using N-Halogen-succinimides,” *ACS Appl. Mater. Inter.*, 15, 55139–55149 (2023).

³ L.A. Ogunfowora, I. Singh, N. Arellano, T.G. Pattison, T. Magbitang, K. Nguyen, B. Ransom, K. Lionti, S. Nguyen, T. Topura, E. Delenia, M. Sherwood, B.M. Savoie, and R. Wojtecki, “Reactive Vapor-Phase Inhibitors for Area-Selective Depositions at Tunable Critical Dimensions,” *ACS Appl. Mater. Inter.* 16(4), 5268–5277 (2024).

⁴ A. Mameli, and A. V. Teplyakov, “Selection Criteria for Small-Molecule Inhibitors in Area-Selective Atomic Layer Deposition: Fundamental Surface Chemistry Considerations,” *Acc. Chem. Res.* 56(15), 2084–2095 (2023).

⁵ I.K. Oh, A.I. Khan, S. Qin, Y. Lee, H.S.P. Wong, E. Pop, and S.F. Bent, “Area-Selective Atomic Layer Deposition for Resistive Random-Access Memory Devices,” *ACS Appl. Mater. Inter.* 15(36), 43087–43093 (2023).

⁶ R. Chen, H. Kim, P.C. McIntyre, and S.F. Bent, “Investigation of self-assembled monolayer resists for hafnium dioxide atomic layer deposition,” *Chem. Mater.* 17(3), 536–544 (2005).

⁷ P. Yu, M.J.M. Merkx, I. Tezsevin, P.C. Lemaire, D.M. Hausmann, T.E. Sandoval, W.M.M. Kessels, and A.J.M. Mackus, “Blocking mechanisms in area-selective ALD by small molecule inhibitors of different sizes: Steric shielding versus chemical passivation,” *Appl. Surf. Sci.* 665, 160141 (2024).

⁸ H. Saare, G. Dianat, and G.N. Parsons, “Comparative in Situ Study of the Initial Growth Trends of Atomic Layer-Deposited Al₂O₃ Films,” *J. Phys. Chem. C* 126(16), 7036–7046 (2022).

⁹ S. Rivillon, Y.J. Chabal, L.J. Webb, D.J. Michalak, N.S. Lewis, M.D. Halls, and K. Raghavachari, “Chlorination of hydrogen-terminated silicon (111) surfaces,” *J. Vac. Sci. & Technol. A* 23(4), 1100–1106 (2005).

¹⁰ T. Parke, D. Silva-Quinones, G.T. Wang, and A. V. Teplyakov, “The Effect of Surface Terminations on the Initial Stages of TiO₂ Deposition on Functionalized Silicon,” *ChemPhysChem* 24(7), e202200724 (2023).

¹¹ E. Frederick, K.J. Dwyer, G.T. Wang, S. Misra, and R.E. Butera, “The stability of Cl-, Br-, and I-passivated Si(100)-(2 × 1) in ambient environments for atomically-precise pattern preservation,” *J. Phys.-Condens. Mat.* 33(44), 444001 (2021).

¹² N. Batra, Vandana, S. Kumar, M. Sharma, S.K. Srivastava, P. Sharma, and P.K. Singh, “A comparative study of silicon surface passivation using ethanolic iodine and bromine solutions,” *Sol. Energ. Mat. and Solar Cells* 100, 43–47 (2012).

¹³ F. Tian, D. Yang, R.L. Opila, and A. V. Teplyakov, “Chemical and electrical passivation of Si(111) surfaces,” *Appl. Surf. Sci.* 258(7), 3019–3026 (2012).

¹⁴ B.J. Eves, and G.P. Lopinski, “Formation and reactivity of high quality halogen terminated Si(111) surfaces,” *Surf. Sci.* 579(2–3), 89–96 (2005).

¹⁵ J. He, S.N. Patitsas, K.F. Preston, R.A. Wolkow, and D.D.M. Wayner, “Covalent Bonding of Thiophenes to Si(111) by a Halogenationrthienylation Route,” *Chem. Phys. Lett.* 286, 508–514 (1998).

¹⁶ T. L. Cottrell, “The Strengths of Chemical Bonds”, 2d ed., Butterworth, London, 1958.

¹⁷ D. Silva-Quinones, C. He, K.J. Dwyer, R.E. Butera, G.T. Wang, and A. V. Teplyakov, “Reaction of hydrazine with solution- And vacuum-prepared selectively terminated Si(100) surfaces: Pathways to the formation of direct Si-N bonds,” *Langmuir* 36(43), 12866–12876 (2020).

¹⁸ K. Sekar, G. Kuri, D.P. Mahapatra, B.N. Dev, J. V Ramana, S. Kumar, and V.S. Raju, “X-Ray Photoelectron Spectroscopic Study of Si(111) and Si(100) Surfaces with Chemically Adsorbed Bromine,” *Surf. Sci.*, 302, 25-36 (1994).

¹⁹ Werner Ker, “The Evolution of Silicon Wafer Cleaning Technology,” *J. Electrochem. Sci.*, 137(6), 1887-1892 (1990).

²⁰ M.J. Frisch, G.W. Trucks, H.B. Schlegel, M.A. Scuseria G E and Robb, J.R. Cheeseman, G. Scalmani, V. Barone, G.A. Petersson, H. Nakatsuji, X. Li, M. Caricato, A. V Marenich, J. Bloino, B.G. Janesko, R. Gomperts, B. Mennucci, H.P. Hratchian, J. V Ortiz, J.L. Izmaylov A F and Sonnenberg, Williams, F. Ding, F. Lipparini F and Egidi, J. Goings, B. Peng, A. Petrone, T. Henderson, D. Ranasinghe, V.G. Zakrzewski, J. Gao, N. Rega, G. Zheng, W. Liang, M. Hada, M. Ehara, K. Toyota, R. Fukuda, J. Hasegawa, M. Ishida, T. Nakajima, Y. Honda, O. Kitao, H. Nakai, K. Vreven T and Throssell, J.A. Montgomery Jr, J.E. Peralta, F. Ogliaro, M.J. Bearpark, J.J. Heyd, E.N. Brothers, K.N. Kudin, V.N. Staroverov, T.A. Keith, R. Kobayashi, J. Normand, K. Raghavachari, A.P. Rendell, S.S. Burant J C and Iyengar, J. Tomasi, M. Cossi, J.M. Millam, M. Klene, C. Adamo, R. Cammi, J.W. Ochterski, R.L. Martin, K. Morokuma, O. Farkas, J.B. Foresman, and D.J. Fox, “Gaussian 16 Rev. C.01,” (2016).

²¹ C. Lee, W. Yang, and R.G. Parr, “Development of the Colic-Salvetti Correlation-Energy Formula into a Functional of the Electron Density,” *Phys. Rev. B* 37(2), 785-789 (1988).

²² A.D. Becke, “A new mixing of Hartree-Fock and local density-functional theories,” *J. Chem. Phys.* 98(2), 1372–1377 (1993).

²³ S. Dunuwila, S. Bai, C.M. Quinn, M.S. Chinn, and A. V. Teplyakov, “Adsorption of β -diketones on a surface of ZnO nanopowder: Dependence of the adsorbate on the diketone structure,” *Surf. Sci.* 749, 122554 (2024).

²⁴ D. Silva-Quinones, R.E. Butera, G.T. Wang, and A. V. Teplyakov, “Solution Chemistry to Control Boron-Containing Monolayers on Silicon: Reactions of Boric Acid and 4-Fluorophenylboronic Acid with H- and Cl-terminated Si(100),” *Langmuir* 37(23), 7194–7202 (2021).

²⁵ H. Jin, C.R. Kinser, P.A. Bertin, D.E. Kramer, J.A. Libera, M.C. Hersam, S.T. Nguyen, and M.J. Bedzyk, “X-ray studies of self-assembled organic monolayers grown on hydrogen-terminated Si(111),” *Langmuir* 20(15), 6252–6258 (2004).

²⁶ S.R. Narayan, J.M. Day, H.L. Thinakaran, N. Herbots, M.E. Bertram, C.E. Cornejo, T.C. Diaz, K.L. Kavanagh, R.J. Culbertson, F.J. Ark, S. Ram, M.W. Mangus, and R. Islam, “Comparative Study of Surface Energies of Native Oxides of Si(100) and Si(111) via Three Liquid Contact Angle Analysis,” in *MRS Adv.*, (2018), pp. 3379–3390.

²⁷ R. Methaapanon, and S.F. Bent, “Comparative study of titanium dioxide atomic layer deposition on silicon dioxide and hydrogen-terminated silicon,” *J. Phys. Chem. C* 114(23), 10498–10504 (2010).

²⁸ D. Silva-Quinones, J.R. Mason, R. Norden, and A. V. Teplyakov, “Inhibition of atomic layer deposition of TiO₂ by functionalizing silicon surface with 4-fluorophenylboronic acid,” *J. Vac. Sci. & Technol. A* 42(3), (2024).

²⁹ C. Ni, Z. Zhang, M. Wells, T.P. Beebe, L. Pirolli, L.P. Méndez De Leo, and A. V. Teplyakov, “Effect of film thickness and the presence of surface fluorine on the structure of a thin barrier film

deposited from tetrakis-(dimethylamino)-titanium onto a Si(100)-2 × 1 substrate,” *Thin Solid Films* 515(5), 3030–3039 (2007).